Journal of Polymer Science

WILEY

JOURNAL OF POLYMER SCIENCE

RESEARCH ARTICLE OPEN ACCESS

Synthesis and Metal Ion Adsorption Properties of a Dense Triazole Polymer Carrying Cysteine Residues

Ryo Ejima[1] | Masaki Nakahata[1] | Yuri Kamon[1,2] | Akihito Hashidzume[1]

[1]Department of Macromolecular Science, Graduate School of Science, Osaka University, Osaka, Japan | [2]Administrative Department, Graduate School of Science, Osaka University, Osaka, Japan

Correspondence: Akihito Hashidzume (hashidzume@chem.sci.osaka-u.ac.jp)

Received: 28 August 2024 | **Revised:** 28 December 2024 | **Accepted:** 27 January 2025

Funding: This work was supported by Japan Society for the Promotion of Science, JP19H05719 and JP24K08510.

Keywords: copper(I)-catalyzed azide–alkyne cycloaddition | cysteine | dense triazole polymers | metal ion adsorption

ABSTRACT

Copper(I)-catalyzed azide–alkyne cycloaddition (CuAAC) is promising as a reaction to synthesize functional polymers consisting of 1,2,3-triazole units. Recently, we reported a series of dense 1,2,3-triazole polymers of 4-azido-5-hexynoic acid derivatives. Herein, we designed a new water-soluble dense 1,2,3-triazole polymer carrying amino acid residues in the side chains, that is, poly(*N*-(4-azido-5-hexynoyl)cysteine) (poly(AC)), bearing L-cysteine as a ligand for metal ions. CuAAC polymerization of a protected monomer followed by deprotection and neutralization yielded the sodium salt of poly(AC) (poly(AC)Na). The adsorption capacity of poly(AC)Na with Cd^{2+} was investigated with a colorimetric assay. Furthermore, the interactions for poly(AC) with group 12 metal ions (Zn^{2+}, Cd^{2+}, and Hg^{2+}) were investigated using isothermal titration calorimetry (ITC) and transmittance measurements. Utilizing the colorimetric assay data, the Cd^{2+} adsorption capacity per unit weight of poly(AC)Na was evaluated to be 4–5 mmol g^{-1}, comparable to those of Cd^{2+} adsorbents reported previously. The ITC data demonstrated that the interactions of poly(AC)Na with Zn^{2+}, Cd^{2+}, and Hg^{2+} were predominantly exothermic. Based on the ITC data, apparent dissociation constants of interactions were roughly estimated to be in the order of 10^{-5}–10^{-4} M, which are comparable to those for metal-binding biomolecules. The transmittance data indicated that the poly(AC)Na/$CdCl_2$ system underwent phase separation.

1 | Introduction

Click chemistry [1] has been utilized in a variety of fields, for example, organic synthesis [2], bioconjugation [3], and polymerization [4]. Copper(I)-catalyzed azide–alkyne cycloaddition (CuAAC) is one of the most useful reactions in click chemistry, which has been widely used for connecting a wide variety of organic skeletons [5], modification of biomolecules with functional groups [6, 7], and synthesis of polymers with well-defined structures [8–13]. Aiming at the synthesis of polymers with well-defined structures like proteins, our group has been focusing on CuAAC polymerization of 3-azido-1-propyne (AP) derivatives [14, 15], which possess azide and alkyne moieties linked with a carbon atom, to obtain dense triazole polymers. Yamasaki et al. [16] synthesized a monomer possessing a *t*-butyl carboxylate group, that is, *t*-butyl 4-azido-5-hexynoate (tBuAH). The CuAAC polymerization of the monomer yielded poly(tBuAH) of $M_w = 1.6 \times 10^4$, which is soluble in common organic solvents. We have synthesized a series of dense triazole oligomers [17] and polymers derived from 4-azido-5-hexynoate (AH) derivatives with various functional groups (e.g., carboxylic acid [18], amide [19], amine [20], hydroxy [20], nitrile [21], and alkyl groups [22]) in the side chains.

In this study, we report a new dense triazole polymer having *N*-substituted amino acid in the side chain. Amino acids are important as building blocks for proteins and are attractive functional groups to be introduced into the side chains of

dense triazole polymers. Figure 1 shows the chemical structure of the polymer used in this study. The monomer unit, *N*-(4-azido-5-hexynoyl)cysteine (AC) is polymerized to yield a polymer (poly(AC)). Poly(AC) is synthesized via CuAAC polymerization of the protected monomer followed by deprotection. Poly(AC) carries 1,2,3-triazole, carboxylic acid, and thiol residues, which can serve as potential coordination sites for metal ions. The interaction of poly(AC) with metal ions in aqueous media is investigated in comparison with those of previously reported dense triazole polymers to clarify the effects of the thiol and carboxylic acid groups: poly(AH) [17] without cysteine thiol and poly(tBuAH) [16] without cysteine thiol and carboxylic acid.

2 | Results and Discussion

2.1 | Synthesis and Characterization of Poly(AC)

Scheme 1 shows the synthesis and polymerization of the monomer used in this study. 4-Azido-6-(*t*-butyldimethylsilyl) -5-hexynoic acid (**1**) was prepared according to the procedure reported previously [16, 19]. Compound **1** was coupled with a protected L-cysteine derivative, *t*-butyl *S*-trityl-L-cysteinate hydrochloride (H-Cys(Trt)-O*t*Bu·HCl) via amide coupling [19] using 1-(3-dimethylaminopropyl)-3-ethylcarbodiimide hydrochloride (EDC) to obtain compound **2**. The *t*-butyldimethylsilyl (TBDMS) protecting group for the alkyne group was then deprotected with tetrabutylammonium fluoride (TBAF) to obtain the monomer (AC^{tBuTrt}, **3**). Compound **2** was characterized by ^1H and ^{13}C NMR spectra (Figures S1, S2, respectively). The ^1H NMR spectrum contains signals ascribable to the protons of trityl groups in the region of 7.4–7.2 ppm. The signals at 4.5 and 4.2 ppm are assignable to the methine protons of cysteine and the TBDMS-AH residue, respectively. The signals in the region of 2.6–1.9 ppm are ascribed to the methylene protons. The spectrum also contains signals due to the methyl protons of TBDMS and *O*-*t*-butyl groups in the region of 1.4–0.1 ppm. Two-dimensional (2D) NMR spectra, that is, correlation spectroscopy (COSY) (Figure S3), heteronuclear single quantum coherence (HSQC) (Figure S4), and heteronuclear multiple bond connectivity (HMBC) (Figure S5) are consistent with the attribution of signals in ^1H and ^{13}C NMR spectra. The electrospray ionization mass spectroscopy (ESI-MS) chart of **2** (Figure S6) shows a signal ascribed to the sodium adduct of **2** at $m/z = 691.3107$ (calcd. 691.3109). AC^{tBuTrt} (**3**) was characterized by ^1H and ^{13}C NMR spectra (Figures S1, S2). The ^1H NMR spectrum contains signals ascribable to the protons of trityl groups in the region of 7.4–7.2 ppm. The signals at 4.5 and 4.2 ppm are assignable to the methine protons of cysteine and the AH residue, respectively. There is a signal due to the ethynyl proton at ca. 2.6 ppm, which overlaps with the signals of methylene protons in the region of 2.6–1.9 ppm. The spectrum contains signals due to the methyl protons of *O*-*t*-butyl groups at 1.4 ppm, but no signals due to those of the TBDMS group. The ESI-MS chart of **3** (Figure S6) contains a signal due to the sodium adduct of **3** at $m/z = 577.2252$ (calcd. 577.2244). These observations are indicative of the successful synthesis of the monomer.

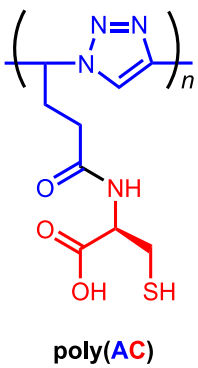

FIGURE 1 | Chemical structure of poly(AC).

AC^{tBuTrt} was then polymerized by CuAAC to obtain a dense triazole polymer carrying protected cysteine residues in the side chain (poly(AC^{tBuTrt})). *O*-*t*-Butyl and *S*-trityl groups were then deprotected to yield poly(AC). Figure 2 shows ^1H NMR spectra for AC^{tBuTrt}, poly(AC^{tBuTrt}), and poly(AC). It should be noted here that signal c (the methine proton in AC^{tBuTrt}) in the top spectrum was observed at $\delta = 4.5$ ppm, whereas signal c (the methine proton in poly(AC^{tBuTrt})) in the middle spectrum was observed at a lower magnetic field ($\delta = 6.0$ ppm), indicative of successful CuAAC polymerization [16]. The ^1H NMR spectrum for the sample deprotected contains almost no signals ascribable to *O*-*t*-butyl ($\delta = 1.2$ ppm) and *S*-trityl ($\delta = 7.4–6.9$ ppm) groups, indicating that the deprotection reactions proceeded quantitatively (90% for *O*-*t*-butyl and 99% for *S*-trityl). The ^{13}C NMR spectrum (Figure S8) exhibits signals ascribable to the carbonyl carbons in the region of 182–172 ppm. Signals due to the 1,2,3-triazole carbons are observed at ca. 145 and 122 ppm. There are signals assignable to the methine and methylene carbons in the region of 65–25 ppm. These observations are indicative of the formation of poly(AC). The poly(AC) sample was then dialyzed against water and neutralized using sodium hydroxide (NaOH) to obtain a water-soluble polyanion in the form of sodium salt (poly(AC)Na). The M_w values were determined to be 1.6×10^4 and 2.7×10^4 for poly(AC) and poly(AC)Na, respectively, by size exclusion chromatography (SEC) measurements (Figure S9). These values indicate no significant difference in the M_w of non-neutralized and neutralized samples. It was not possible to remove the Cu catalyst completely by the chelating agent, for example, tetrasodium ethylenediaminetetraacetate (EDTA·4Na) and *N*,*N*,*N*′,*N*″,*N*″-pentamethyldiethylenetriamine (PMDETA) (data not shown) [16, 19]. As the experimental section described, the elemental analysis data exhibited that the poly(AC) sample contained ca. 10 mol% Cu ion per monomer unit, indicating that ca. 90% of the AC units are free from Cu ions. Thus, it is likely that there was only a small effect of the residual Cu ions on the results reported in the following subsections.

2.2 | Cd^{2+} Adsorption Capability and Loading Capacity

The interactions of poly(AC) with metal ions were studied in terms of the adsorption of metal ions to the polymer in aqueous solutions. Here, the interactions of the poly(AC)Na and poly(AH)Na samples with Cd^{2+} were investigated by estimating the Cd^{2+} removal capability and loading capacity of the polymer samples using a colorimetric assay (Figure 3). The

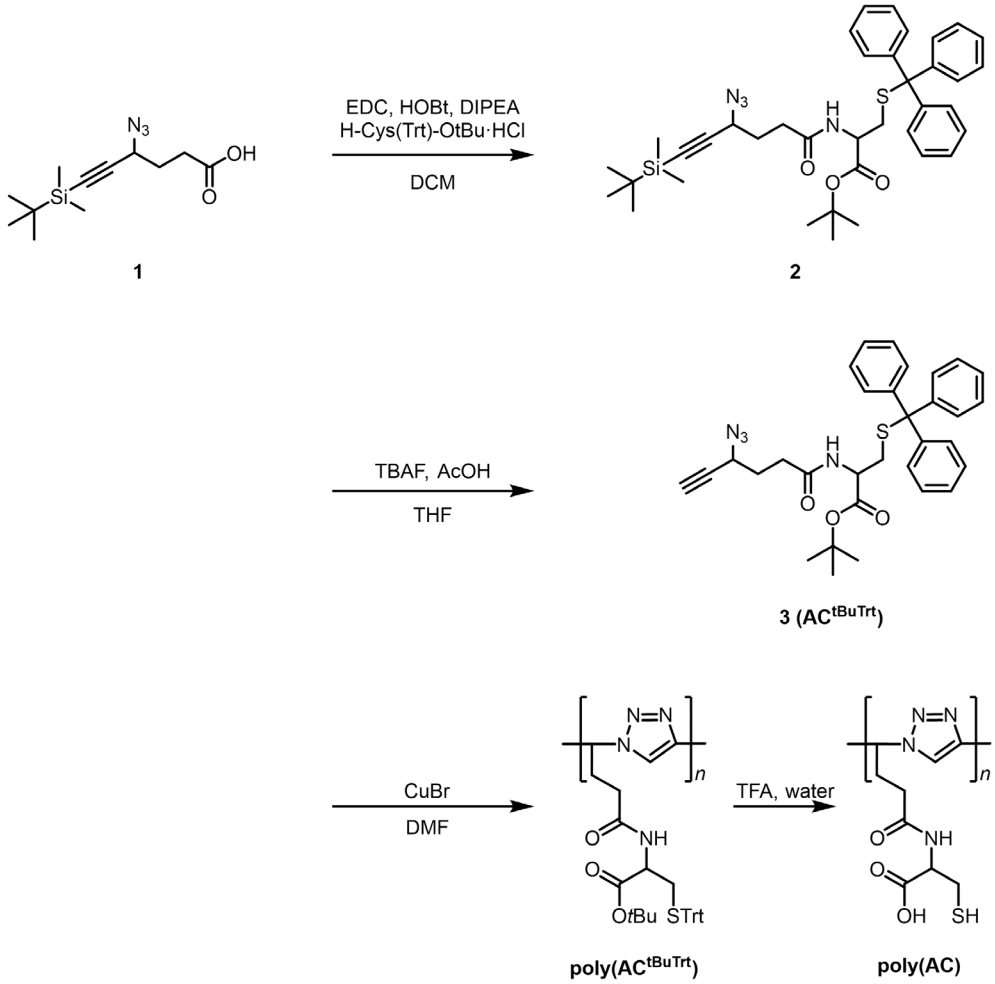

SCHEME 1 | Synthesis of *t*-butyl *N*-(4-azido-5-hexynoyl)-*S*-tritylcysteine (AC^{tBuTrt} (**3**)) and CuAAC polymerization of **3** followed by deprotection to obtain poly(AC).

amount of Cd^{2+} adsorbed was evaluated using poly(AC)Na, poly(AH)Na, and poly(tBuAH) [16] (Figure 3a). As shown in Figure 3b, a solution of poly(AC)Na or poly(AH)Na, or a suspension of poly(tBuAH) was mixed with a Tris–HCl buffer (10 mM, pH 7.4) containing Cd^{2+}, followed by stirring for 1 h and centrifugation at 3500 rpm in the ultrafiltration device (MWCO = 1 kDa). It should be noted here that almost no polymer chains passed through the filter under these conditions (Figure S10). The molar concentration of Cd^{2+} (C_{Cd}) in the filtrate was determined using a colorimetric assay based on cadion as a Cd^{2+}-specific dye. Plots in Figure 3c demonstrate C_{Cd} in the filtrate after the ultrafiltration of a mixed solution in the absence and presence of poly(AC)Na, poly(AH)Na (0.0001, 0.001, 0.01, and 0.1 g L^{-1}), or poly(tBuAH) (0.1 g L^{-1}). As can be seen in the plots, C_{Cd} in the filtrate is smaller at a higher polymer concentration, indicative of the adsorption of Cd^{2+} to the polymer samples. The bar graphs in Figure 3d display the molar amount of Cd^{2+} adsorbed per unit weight (q_{Cd} in mmol g^{-1}, see Figure S11 for calculation) of the polymer samples. This graph indicates that the maximum values for poly(AC)Na and poly(AH)Na (q_{Cd} = 4.8 and 10 mmol g^{-1}, respectively) at C_p = 0.0001 g L^{-1} are comparable to or larger than those reported to date for other bio-based [23–26], inorganic [27–30], organic [31–34], and hybrid materials [35–41]. It is noteworthy that the q_{Cd} value for poly(AH)Na is higher than that of zeolite nanoparticles coupled to poly(vinyl alcohol) nanofibers (7.5 mmol g^{-1}) [42], which is the largest adsorption capacity to date [43]. On the other hand, Cd^{2+} ions were removed completely at $C_p \geq 0.1$ g L^{-1}. This C_p value is comparable to those of previous works [43, 44].

To discuss from a molecular perspective, the amount of Cd^{2+} adsorbed per monomer unit (q'_{Cd} in mol mol^{-1}) was estimated by multiplying q_{Cd} (in mmol g^{-1}) by the molar mass of the monomer unit (Figure 3e). The q'_{Cd} value of poly(AH)Na was larger than that of poly(AC)Na. It should be noted here that these q'_{Cd} values are higher than the ratios of Cd^{2+} to the monomer unit at which the charge of Cd^{2+} is neutralized by the thiolate and carboxylate residues (1 for poly(AC)Na and 0.5 for poly(AH)Na). These data indicate that not only thiol and carboxylic acid residues but also 1,2,3-triazole residues serve as metal binding sites [45].

2.3 | Isothermal Titration Calorimetry (ITC) Measurements

Since the colorimetric assay data were indicative of the interactions of poly(AC)Na samples with Cd^{2+}, the interaction

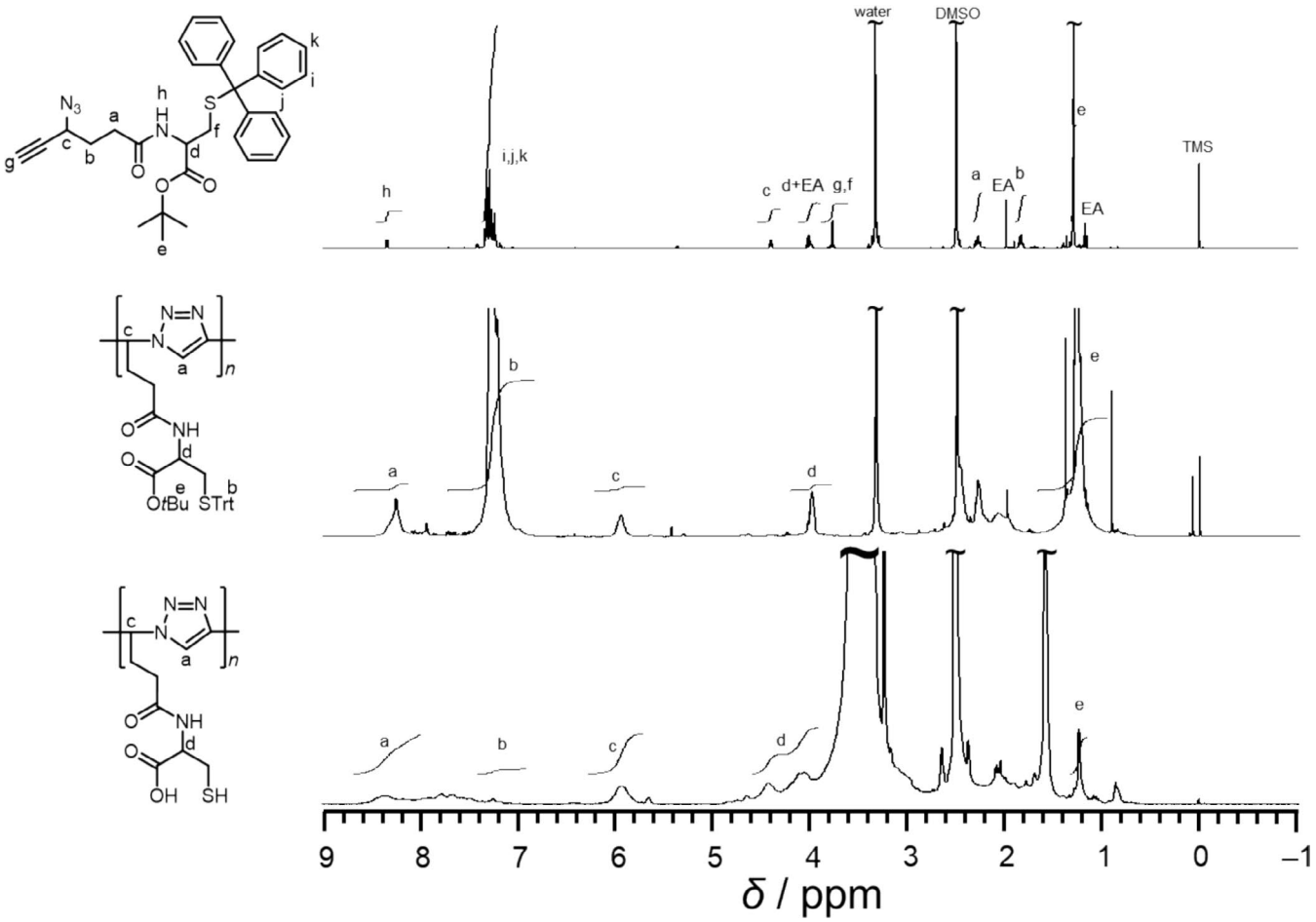

FIGURE 2 | ^{1}H NMR spectra for AC^{tBuTrt} (top), poly(AC^{tBuTrt}) (middle), and poly(AC) (bottom) (DMSO-d_6). EA: ethyl acetate.

of poly(AC)Na with metal ions was investigated by ITC from the thermodynamic perspective. Here we chose divalent metal ions of group 12 elements (Zn^{2+}, Cd^{2+}, and Hg^{2+}). It is known that Zn is an essential metal element, whereas Cd and Hg are highly toxic heavy metal elements [46]. Figure 4 shows plots of the additional thermal power (dQ/dt) against time and of the enthalpy change (ΔH) against the molar ratio of metal ion/monomer unit (r) obtained by the ITC data for poly(AC)Na (Figure 4a) and poly(AH)Na (Figure 4b) titrated with 10 mM MCl_2 (M = Zn, Cd, and Hg) in a Tris–HCl buffer (10 mM, pH 7.4). The ΔH data were fitted using the one or two independent model. Table 1 summarizes the interaction parameters obtained. Notably, the data for poly(AC)Na titrated with $ZnCl_2$ and $CdCl_2$ were fitted using site #1 with a negative ΔH (exothermic, i.e., enthalpy-driven) in the former stage and site #2 with a positive ΔH (endothermic, i.e., entropy-driven) in the latter stage. The data for $HgCl_2$ were fitted using site #1 with a negative ΔH (exothermic). In the enthalpy-driven process, poly(AC) chains may adsorb Zn^{2+}, Cd^{2+}, and Hg^{2+} ions through electrostatic interaction. In the entropy-driven process, on the other hand, counterions and hydrated water molecules may be released from poly(AC) chains upon interaction with Zn^{2+} and Cd^{2+} ions, followed by intra- and interpolymer aggregations. It should be noted here that the apparent K_D values for poly(AC) with Zn^{2+} and Hg^{2+} are in the order of 10^{-5}–10^{-4} M, which are larger than those for phytochelatin, metal ion-binding polypeptides (γGlu-Cys)$_n$-Gly (n = 2–11) used by plants [47], and those for phytochelatin analogs, for example, (αGlu-Cys)$_4$-Gly [48]. The apparent K_D values for poly(AC) are comparable to those for glutathione [47], a monomer of phytochelatin, and random peptides mimicking phytochelatin, oligo(Glu-*co*-Cys) [49].

The interactions of poly(AC)Na with metal ions are compared with those of poly(AH)Na [18] to clarify the effect of the thiol group in the cysteine residue. (Here, poly(tBuAH) [16] was not used due to its poor solubility in water.) The ΔH data for poly(AH)Na titrated with $ZnCl_2$, $CdCl_2$, and $HgCl_2$ were fitted using the two independent models. Table 1 also summarizes the interaction parameters obtained. Notably, the ΔH values for sites #1 and #2 are negative (exothermic) and positive (endothermic) for $ZnCl_2$, $CdCl_2$, and $HgCl_2$.

Intriguingly, the interaction of poly(AC)Na with Hg^{2+} does not involve an endothermic (entropy-driven) process. It is thus likely that poly(AC)Na chains capture Hg^{2+} through the electrostatic interaction of free carboxylate and thiolate groups with these ions. Notably, the titration curves for the poly(AC)Na/$HgCl_2$ and poly(AH)Na/$HgCl_2$ systems show spikes throughout the titration. This is presumably because of the larger heat of dilution for $HgCl_2$ compared to those for $ZnCl_2$ and $CdCl_2$ in a Tris–HCl buffer (Figure S12), which causes excess heat feedback from the ITC system. Overall, the calorimetric data supported that both poly(AC)Na and

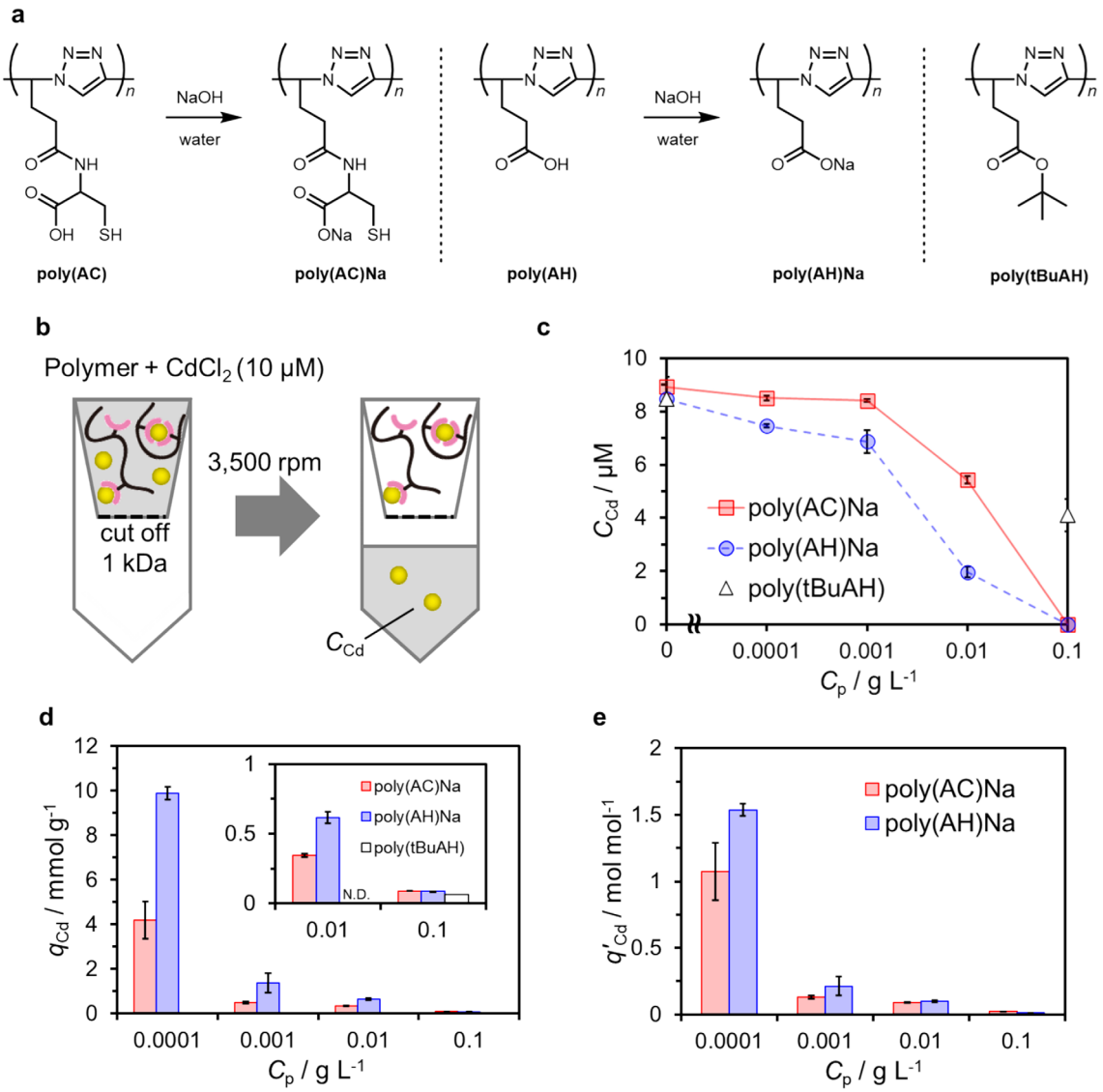

FIGURE 3 | (a) Chemical structures of polymers for Cd^{2+} ion adsorption measurements. (b) Schematic illustration of the ultrafiltration experiments and colorimetric assay to determine the Cd^{2+} concentration in the filtrate. (c) The concentration of Cd^{2+} in the filtrate (C_{Cd}) and (d) the amount of Cd^{2+} bound to 1 g of polymer (q_{Cd}) for poly(AC)Na, poly(AH)Na and poly(tBuAH) as a function of polymer concentration (C_p). (e) The number of Cd^{2+} bound to the monomer unit (q'_{Cd}) for poly(AC)Na and poly(AH)Na as a function of C_p.

poly(AH)Na interact with Zn^{2+}, Cd^{2+}, and Hg^{2+}. The interactions of poly(AH)Na with the metal ions are predominantly endothermic, whereas the interaction of poly(AC)Na are predominantly exothermic.

2.4 | Transmittance Measurements

The interactions of poly(AC)Na and poly(AH)Na with Zn^{2+}, Cd^{2+}, and Hg^{2+} were also studied by transmittance measurements in a Tris–HCl buffer (10 mM, pH 7.4). Figure 5 shows the transmittance at 500 nm ($\%T_{500}$) for the poly(AC)Na/MCl_2 and poly(AH)Na/MCl_2 systems as a function of r (i.e., the molar ratio of metal ion/monomer unit). Here the concentration of the polymer was fixed at 0.80 g L^{-1} (2.9 and 4.6 mM for AC and AH units, respectively). In the poly(AC)Na/$ZnCl_2$ system (Figure 5a), $\%T_{500}$ is almost constant independent of r. In the poly(AC)Na/$CdCl_2$ and poly(AC)Na/$HgCl_2$ systems (Figure 5a), on the other hand, $\%T_{500}$ decreases with r. These observations indicate that interpolymer aggregates were formed through complexation of poly(AC)Na with Cd^{2+} and Hg^{2+}. It should be noted here that $\%T_{500}$ commences to decrease rapidly at $r \sim 0.3$ for the poly(AC)Na/$CdCl_2$ system. The $\%T_{500}$ decrease is indicative of phase separation at $r > 0.3$, in which the endothermic event was observed in the ITC measurement. In the poly(AH)Na/$ZnCl_2$ system (Figure 5b), $\%T_{500}$ commences to decrease significantly at $r \sim 0.2$, indicative of phase separation at $r > 0.2$. In the poly(AH)Na/$CdCl_2$ and poly(AH)Na/$HgCl_2$ systems (Figure 5b), on the other hand, $\%T_{500}$ seems to decrease slightly with r.

3 | Conclusion

In this study, we have designed and synthesized a new dense triazole polymer with cysteine in the side chains. The water-soluble

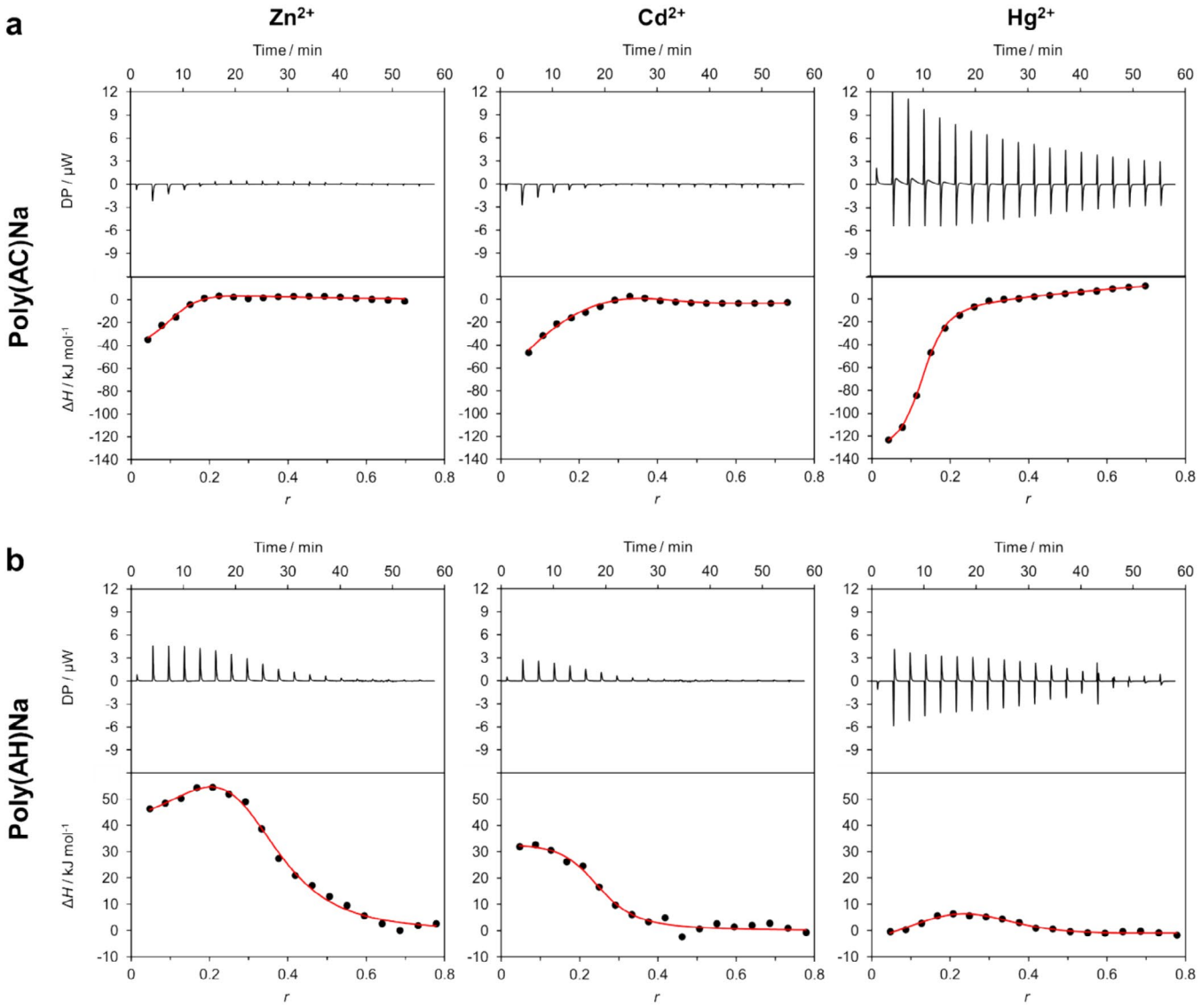

FIGURE 4 | Plots of differential thermal power (dQ/dt, DP) versus time and enthalpy (ΔH) versus the molar ratio (r) of metal ions versus monomer unit by titrating (a) poly(AC)Na (0.80 g L^{-1}) or (b) poly(AH)Na (0.40 g L^{-1}) in the cell with $ZnCl_2$ (10 mM), $CdCl_2$ (10 mM), or $HgCl_2$ (10 mM) in the syringe. The best-fit curves for ΔH data using the one or two independent models are shown (solid red lines).

polymer, poly(AC)Na, was obtained by CuAAC polymerization of the monomer carrying *N*-substituted cysteine with protected thiol and carboxylic acid groups, followed by deprotection and neutralization. The interactions of poly(AC)Na with Cd^{2+} ions and group 12 metal ions (Zn^{2+}, Cd^{2+}, and Hg^{2+}) in aqueous solutions were investigated using the colorimetric assay and ITC measurements, respectively. The maximum values of Cd^{2+} adsorption capacity (q_{Cd}) for both the poly(AC)Na and poly(AH)Na samples were comparable to or higher than those for the Cd^{2+} adsorption materials reported previously, whereas the amount needed for complete removal of Cd^{2+} ions was comparable to those of previous works. The number of Cd^{2+} ions adsorbed per monomer unit was larger than that predicted for simple metal–ligand (thiol and carboxylate) interactions, indicating that not only the cysteine residues but also the dense triazole polymer backbone serves as binding sites for Cd^{2+} ions. The ITC data indicated that the interactions of poly(AC)Na with metal ions were predominantly exothermic, contrasting with those of poly(AH)Na, which carries no cysteine thiol groups. The transmittance data indicated that phase separation occurred upon the complexation of poly(AC)Na with Cd^{2+} and poly(AH)Na with Zn^{2+}, respectively.

4 | Experimental Section

4.1 | Measurements

^1H, ^{13}C, and 2D (COSY, HSQC, HMBC) NMR measurements were carried out on a JEOL JNM ECA500, ECS400, or Bruker AVANCE NEO 700 spectrometer at 25°C using chloroform-*d* ($CDCl_3$), deuterium oxide (D_2O) or dimethyl sulfoxide-d_6 (DMSO-d_6) as a solvent. Chemical shifts were referenced to the signal due to tetramethylsilane (0 ppm for ^1H and ^{13}C) for $CDCl_3$ and DMSO-d_6, and to the signal due to HOD for D_2O (4.79 ppm at 25°C and 4.31 ppm at 70°C). MS data were obtained on a ThermoFisher Scientific Orbitrap XL using an ESI source. Methanol was used as a solvent. Internal calibration

TABLE 1 | Fitting parameters determined using the ITC data in Figure 4.

Polymer/metal ion	Site #1				Site #2			
	K_D/M	N	ΔH/kJ mol^{-1}	ΔS/J mol^{-1} K^{-1}	K_D/M	N	ΔH/kJ mol^{-1}	ΔS/J mol^{-1} K^{-1}
Poly(AC)Na/Zn^{2+}	5.5×10^{-5}	0.10	−3.4	70	2.6×10^{-4}	0.19	14	73
Poly(AC)Na/Cd^{2+}	3.5×10^{-4}	0.14	−8.7	37	5.8×10^{-5}	0.40	1.7	87
Poly(AC)Na/Hg^{2+}	2.7×10^{-5}	0.11	−4.8	72	—	—	—	—
Poly(AH)Na/Zn^{2+}	1.1×10^{-4}	0.28	−18	15	8.8×10^{-5}	0.31	20	1.4×10^{2}
Poly(AH)Na/Cd^{2+}	2.3×10^{-5}	0.29	−7.2	65	2.5×10^{-5}	0.21	9.0	1.2×10^{2}
Poly(AH)Na/Hg^{2+}	1.4×10^{-4}	0.29	−47	−85	1.3×10^{-4}	0.29	47	2.3×10^{2}

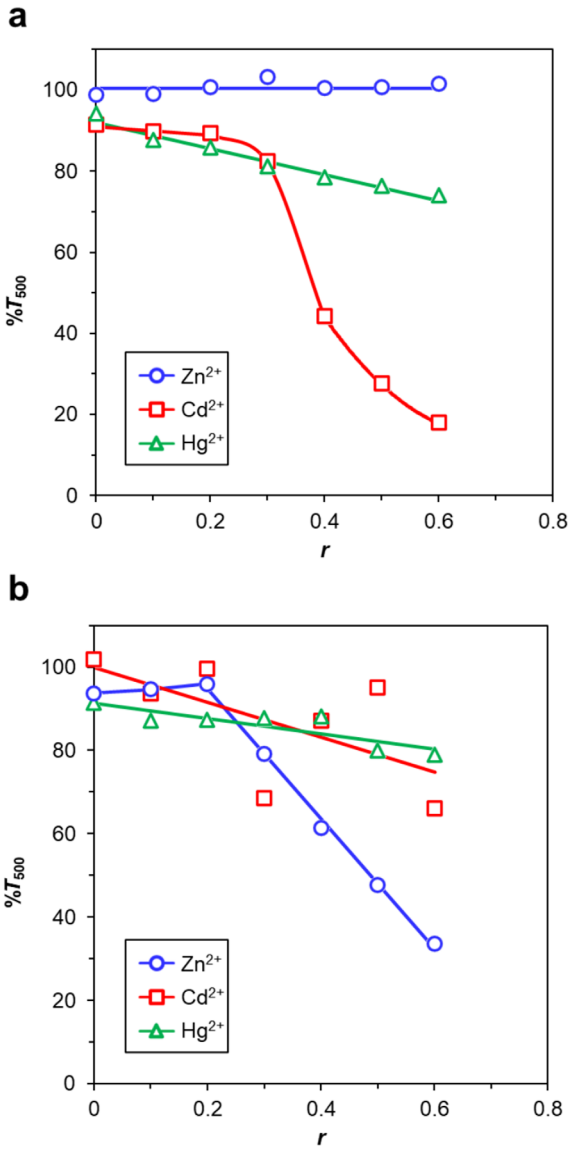

FIGURE 5 | Transmittance at $\lambda = 500$ nm ($\%T_{500}$) for (a) the poly(AC)Na/MCl_2 and (b) poly(AH)Na/MCl_2 systems as a function of r, the molar ratio of metal ion/monomer unit, in a Tris–HCl buffer (10 mM, pH 7.4). The polymer concentration was fixed at 0.80 g L^{-1} (2.9 and 4.6 mM for AC and AH units, respectively). M = Zn (blue circle), Cd (red square), and Hg (green triangle).

of ESI-MS was carried out using the monoisotopic peaks of sodium adducted ion of diethylphthalate (m/z 314.1410), protonated ion of di-2-ethylhexylphthalate (m/z 391.2843), and sodium adducted ion of di-2-ethylhexylphthalate (m/z 413.2662). SEC experiments were carried out at 25°C on an HPLC system (CBM-20A/LC-20 AD/SIL-10AXL/DGU-20A3R/CTO-20 AC/RID-20A (Shimadzu, Kyoto, Japan)) equipped with an Asahipak GF-1G 7B guard column and an Asahipak GF-7 M HQ column (Resonac, Tokyo, Japan), using a Tris–HCl buffer (10 mM) as the eluent at a flow rate of 0.7 mL min^{-1}. The molecular weights were calibrated with the ReadyCal-Kit poly(ethylene glycol (PEG)/poly(ethylene oxide) (PEO) (PSS Polymer Standards Service GmbH, Mainz, Germany). Sample solutions were filtered with a DISMIC-13HP PTFE 0.20 μm filter just prior to injection. ITC measurements were carried out with a MicroCal PEAQ-ITC using aqueous solutions using a Tris–HCl buffer (10 mM, pH 7.4) as a solvent. The ITC data were analyzed using the Nanoanalyze software (TA instruments, New Castle, DE, USA). Adsorption of Cd^{2+} to the polymer in solution was investigated as follows. A Tris–HCl buffer solution (10 mM, pH 7.4) containing polymer and $CdCl_2$ was stirred for 1 h and was filtered through an ultrafiltration device (molecular weight cut off (MWCO) = 1 kDa). The concentration of Cd^{2+} in the filtrate was determined according to the protocol of the Spectroquant Cadmium Test kit (Merck, Darmstadt, Germany) using a Spectroquant Prove 600 UV-visible spectrophotometer (Merck, Darmstadt, Germany). Transmittance measurements were carried out with a UV-2600 spectrometer (Shimadzu, Kyoto, Japan) using a 1.0 cm path length quartz cuvette.

4.2 | Materials

Hexane, diethyl ether, ethyl acetate, tetrahydrofuran (THF), dimethyl sulfoxide (DMSO), methanol, acetic acid (AcOH), aqueous HCl (1 M), NaOH, $ZnCl_2$, $CdCl_2$, $HgCl_2$, tris(hydroxymethyl)aminomethane, $CDCl_3$, and DMSO-d_6 were purchased from FUJIFILM Wako Pure Chemical Corp. (Osaka, Japan). A solution of TBAF in THF (1 M), EDC, and PMDETA were purchased from Tokyo Chemical Industry Co. Ltd. (Tokyo, Japan). Citric acid, *N*,*N*-diisopropylethylamine (DIPEA), 1-hydroxybenzotriazole (HOBt), trifluoroacetic acid (TFA), dichloromethane (DCM), *N*,*N*-dimethylformamide (DMF), tetrasodium ethylenediaminetetraacetate (EDTA·4Na), sodium

bicarbonate ($NaHCO_3$), sodium chloride (NaCl), sodium sulfate (Na_2SO_4), and copper(I) bromide (CuBr) were purchased from Nacalai Tesque Inc. (Kyoto, Japan). H-Cys(Trt)-O*t*Bu·HCl was purchased from Watanabe Chemical Industries Co. Ltd. (Hiroshima, Japan). All the reagents were used without purification. For thin layer chromatography (TLC) analysis throughout this work, Merck precoated TLC plates (silica gel 60 F254) were used. The products were purified by column chromatography using silica gel 60 (Nacalai Tesque, spherical, neutrality). 4-Azido-6-(*t*-butyldimethylsilyl)-5-hexynoic acid (Scheme 1-1) was prepared according to previous reports [16, 19].

4.3 | Synthesis and Characterization of Monomers and Polymers

4.3.1 | Synthesis of *t*-Butyl *N*-(4-Azido-6-(*t*-Butyldimethylsilyl)-5-Hexynoyl)-*S*-Tritylcysteinate (2)

EDC (88 mg, 0.46 mmol), HOBt (73 mg, 0.48 mmol), and DIPEA (92 μL, 0.53 mmol) were added to a solution of 4-azido-6-(*t*-butyldimethylsilyl)-5-hexynoic acid (**1**) (0.11 g, 0.41 mmol) in DCM (5.0 mL) and the mixture was stirred at 0°C for 15 min. H-Cys(Trt)-O*t*Bu·HCl (0.18 g, 0.40 mmol) was added to the mixture. After stirring at room temperature for 30 h, the organic phase was washed with saturated $NaHCO_3$ (3 × 90 mL), saturated NaCl (3 × 20 mL), and dried with Na_2SO_4. After removing the volatile fractions, the product was purified by column chromatography using a mixed solvent of hexane and ethyl acetate (3/1, v/v) as an eluent. Volatile fractions were removed to obtain **2** as a pale yellow oil (194 mg, 0.29 mmol, 78%). ^{1}H NMR (500 MHz, [D]chloroform, 298 K, TMS): δ 7.43–7.36 (m, 6H, Ar H), 7.33–7.25 (m, 6H, Ar H), 7.25–7.17 (m, 3H, Ar H), 5.94 (dd, J = 7.8, 3.4 Hz, 1H, amide NH), 4.55–4.48 (m, 1H, CH), 4.25–4.21 (m, 1H, CH), 2.63 (dd, J = 12.0, 5.4 Hz, 1H, CH_2), 2.51 (dd, J = 12.0, 4.5 Hz, 1H, CH_2), 2.32 (t, J = 7.3 Hz, 2H, CH_2), 2.06–1.92 (m, 2H, CH_2), 1.44 (s, 9H, CH_3), 0.95 (s, 9H, CH_3), 0.14 (s, 6H, CH_3). HRMS (ESI) *m/z*: $[M+Na]^+$ calcd for $C_{38}H_{48}N_4NaO_3S$, 691.3109; found, 691.3107.

4.3.2 | Synthesis of *t*-Butyl *N*-(4-Azido-5-Hexynoyl)-*S*-Tritylcysteinate (AC^{tBuTrt}, 3)

AcOH (0.23 mL, 4.0 mmol) was added to a solution of **2** (2.66 g, 3.98 mmol) in THF (70 mL) at −20°C under a nitrogen atmosphere. The solution was stirred for 10 min, and a solution of TBAF in THF (1 M, 5.3 mL, 5.3 mmol) was added to the solution dropwise. After stirring for 50 min, the reaction mixture was allowed to warm to room temperature with stirring for 21 h. An aqueous solution of 10% citric acid (30 mL) was added to the reaction mixture. The product was extracted with ethyl acetate (3 × 50 mL). The organic phases were combined, and the combined organic layer was washed with saturated $NaHCO_3$ (3 × 10 mL) and saturated NaCl (5.0 mL). The organic layer was dried with Na_2SO_4. After filtration, volatile fractions were removed under reduced pressure. The product was purified by column chromatography using a mixed solvent of hexane and ethyl acetate (4/1–1/1, v/v) as an eluent. After removing the solvents, AC^{tBuTrt} (**3**) was obtained as a pale yellow oil (1.45 g, 2.62 mmol, 66%). ^{1}H NMR (500 MHz, [D]chloroform, 298 K, TMS): δ 7.42–7.32 (m, 6H, Ar H), 7.31–7.22 (m, 6H, Ar H), 7.22–7.15 (m, 3H, Ar H), 5.89 (d, J = 7.8 Hz, 1H, amide NH), 4.52–4.44 (m, 1H, CH), 4.21 (td, J = 6.8, 2.3 Hz, 1H, CH), 2.60 (ddd, J = 12.1, 5.5, 2.9 Hz, 2H, CH_2), 2.56 (d, J = 2.3 Hz, 1H, CH), 2.30 (t, J = 7.4 Hz, 2H, CH_2), 2.04–1.94 (m, 2H, CH_2), 1.41 (s, 9H, CH_3). HRMS (ESI) *m/z*: $[M+Na]^+$ Calcd for $C_{32}H_{34}N_4NaO_3S$, 577.2252; Found, 577.2244.

4.3.3 | Synthesis of Poly(AC^{tBuTrt})

CuBr (53 mg, 0.37 mmol) was added to a solution of AC^{tBuTrt} (1.6 g, 2.8 mmol) in dry DMF (3.8 mL). The reaction solution was stirred at 60°C for 48 h. After the reaction mixture was cooled down to room temperature, the solvent was removed under reduced pressure. The residue was dissolved in ethyl acetate (50 mL) and washed with 0.5 M EDTA·4Na aqueous solution (3 × 50 mL). The organic layer was dried with Na_2SO_4. After filtration, volatile fractions were removed under reduced pressure. The polymer obtained was purified by reprecipitation three times using a pair of DMF (2.0 mL) and diethyl ether (40 mL) as good and poor solvents. After drying under reduced pressure, the polymer was obtained as a brown powder (1.07 g, 67%).

4.3.4 | Synthesis of Poly(AC)Na

TFA (27.5 mL) and water (28.8 μL) were added to poly(AC^{tBuTrt}) (466 mg) and the mixture was stirred at 80°C for 48 h. After the reaction mixture was cooled down to room temperature, the solvent was removed under reduced pressure. The polymer obtained was purified by reprecipitation three times using DMF (2.0 mL) and a mixed solvent of hexane and diethyl ether (1/1, v/v) (40 mL) as good and poor solvents to remove TFA and by-products of deprotection. A Tris–HCl buffer (10 mM, pH 7.4, 10 mL) was added to the precipitate, and the mixture was filtered to extract the water-soluble fraction of the polymer. The filtrate was dialyzed against water using a dialysis membrane (MWCO = 1 kDa) for 14 h. After removing the solvent, poly(AC) was recovered as a dark brown solid. Poly(AC) was mixed with aqueous NaOH (0.1 M, 1.04 mL). After removing the solvent, poly(AC)Na (20 mg, 9%) was obtained. Anal. Calcd for poly(AC) sample: $(C_9H_{12}N_4O_3S)_{0.89}(C_{13}H_{20}N_4O_3S)_{0.1}(C_{28}H_{26}N_4O_3S)_{0.01}(H_2O)_{1.5}(CuO)_{0.1}$: C 38.48, H 5.37, N 18.72; Found: C 38.47, H 4.87, N 16.95 (ash 6.79).

4.3.5 | Neutralization of Poly(AH)

Poly(AH)Na was prepared according to the same procedure as that of poly(AC)Na. Poly(AH) (10.9 mg), aqueous NaOH (0.1 M, 0.71 mL). Yield: 7.7 mg, 62%.

Acknowledgments

This study was partly supported by JSPS KAKENHI (JP19H05719 to M.N. and JP24K08510 to Y.K.). One of the authors (R.E.) was supported by the Program for Leading Graduate Schools: "Interactive Materials Science Cadet Program." The authors thank Prof. Dr. Shinji Sakai, Graduate School of Engineering Science, Osaka University, for providing access to the UV-2600 spectrometer.

References

1. H. C. Kolb, M. G. Finn, and K. B. Sharpless, "Click Chemistry: Diverse Chemical Function From a Few Good Reactions," *Angewandte Chemie International Edition* 40 (2001): 2004–2021.

2. (a) J.-F. Lutz, J.-M. Lehn, E. W. Meijer, and K. Matyjaszewski, "From Precision Polymers to Complex Materials and Systems," *Nature Reviews Materials* 1 (2016): 16024. (b) B. van Genabeek, B. A. G. Lamers, C. J. Hawker, E. W. Meijer, W. R. Gutekunst, and B. V. K. J. Schmidt, "Properties and Applications of Precision Oligomer Materials; Where Organic and Polymer Chemistry Join Forces," *Journal of Polymer Science* 59 (2021): 373–403.

3. C. S. McKay and M. G. Finn, "Click Chemistry in Complex Mixtures: Bioorthogonal Bioconjugation," *Cell Chemical Biology* 21 (2014): 1075–1101.

4. A. Qin and B. Z. Tang, *Click Polymerization* (London, UK: Royal Society of Chemistry, 2018).

5. E. Haldón, M. C. Nicasio, and P. J. Pérez, "Copper-Catalysed Azide–Alkyne Cycloadditions (CuAAC): An Update," *Organic & Biomolecular Chemistry* 13 (2015): 9528–9550.

6. N. J. Agard, J. A. Prescher, and C. R. Bertozzi, "A Strain-Promoted [3 + 2] Azide–Alkyne Cycloaddition for Covalent Modification of Biomolecules in Living Systems," *Journal of the American Chemical Society* 126 (2004): 15046–15047.

7. J. M. Baskin, J. A. Prescher, S. T. Laughlin, et al., "Copper-Free Click Chemistry for Dynamic *in vivo* imaging," *Proceedings of the National Academy of Sciences* 104 (2007): 16793–16797.

8. M. Meldal, "Polymer "Clicking" by CuAAC Reactions," *Macromolecular Rapid Communications* 29 (2008): 1016–1051.

9. N. G. Angelo and P. S. Arora, "Nonpeptidic Foldamers From Amino Acids: Synthesis and Characterization of 1,3-Substituted Triazole Oligomers," *Journal of the American Chemical Society* 127 (2005): 17134–17135.

10. N. G. Angelo and P. S. Arora, "Solution- and Solid-Phase Synthesis of Triazole Oligomers That Display Protein-Like Functionality," *Journal of Organic Chemistry* 72 (2007): 7963–7967.

11. R. Pfukwa, P. H. J. Kouwer, A. E. Rowan, and B. Klumperman, "Templated Hierarchical Self-Assembly of Poly(*p*-aryltriazole) Foldamers," *Angewandte Chemie International Edition* 52 (2013): 11040–11044.

12. H. V. T. Nguyen, Y. Jiang, S. Mohapatra, et al., "Bottlebrush Polymers with Flexible Enantiomeric Side Chains Display Differential Biological Properties," *Nature Chemistry* 14 (2022): 85–93.

13. W. Wang, Y. Jiang, Z. Huang, et al., "Discrete, Chiral Polymer–Insulin Conjugates," *Journal of the American Chemical Society* 144 (2022): 23332–23339.

14. A. Hashidzume, T. Nakamura, and T. Sato, "Copper-Catalyzed Azide-Alkyne Cycloaddition Oligomerization of 3-Azido-1-Propyne Derivatives," *Polymer* 54 (2013): 3448–3451.

15. S. Nakano, A. Hashidzume, and T. Sato, "Quarternization of 3-Azido-1-Propyne Oligomers Obtained by Copper(I)-Catalyzed Azide–Alkyne Cycloaddition Polymerization," *Beilstein Journal of Organic Chemistry* 11 (2015): 1037–1042.

16. S. Yamasaki, Y. Kamon, L. Xu, and A. Hashidzume, "Synthesis of Dense 1,2,3-Triazole Polymers Soluble in Common Organic Solvents," *Polymers* 13 (2021): 1627.

17. Y. Kamon, J. Miura, K. Okuno, S. Yamasaki, M. Nakahata, and A. Hashidzume, "Synthesis of Stereoregular Uniform Oligomers Possessing a Dense 1,2,3-Triazole Backbone," *Macromolecules* 56 (2023): 292–304.

18. L. Xu, Y. Kamon, and A. Hashidzume, "Synthesis of a New Polyanion Possessing Dense 1,2,3-Triazole Backbone," *Polymers* 13 (2021): 1614.

19. K. Okuno, T. Arisawa, Y. Kamon, A. Hashidzume, and F. M. Winnik, "Synthesis of New Thermoresponsive Polymers Possessing the Dense 1,2,3-Triazole Backbone," *Langmuir* 38 (2022): 5156–5165.

20. T. Omae, M. Nakahata, Y. Kamon, and A. Hashidzume, "Synthesis of an Alternating Polycation with the Dense 1, 2, 3-Triazole Backbone," *Synlett* 35 (2024): 1301–1305.

21. L. Xu, M. Nakahata, Y. Kamon, and A. Hashidzume, "Synthesis of an Alternating Copolymer of the Dense 1,2,3-Triazolebackbone Carryingt-Butylester and Nitrile Side Chains," *Journal of Polymer Science* 62 (2024): 937–945.

22. T. Yamamoto, R. Taguchi, Z. Yan, et al., "Interaction of Cyclodextrins with Amphiphilic Alternating Cooligomers Possessing the Dense Triazole Backbone," *Langmuir* 40 (2024): 7178–7191.

23. J. Wątły, M. Łuczkowski, M. Padjasek, and A. Krężel, "Phytochelatins as a Dynamic System for Cd(II) Buffering From the Micro- to Femtomolar Range," *Inorganic Chemistry* 60 (2021): 4657–4675.

24. M. A. Naeem, M. Imran, M. Amjad, et al., "Batch and Column Scale Removal of Cadmium From Water Using Raw and Acid Activated Wheat Straw Biochar," *Water* 11 (2019): 1438.

25. N. Sankararamakrishnan, P. Kumar, and V. S. Chauhan, "Modeling Fixed Bed Column for Cadmium Removal from Electroplating Wastewater," *Separation and Purification Technology* 63 (2008): 213–219.

26. N. Isobe, X. Chen, U.-J. Kim, et al., "TEMPO-Oxidized Cellulose Hydrogel as a High-Capacity and Reusable Heavy Metal Ion Adsorbent," *Journal of Hazardous Materials* 260 (2013): 195–201.

27. L. Panda, S. K. Jena, S. S. Rath, and P. K. Misra, "Heavy Metal Removal from Water by Adsorption Using a Low-Cost Geopolymer," *Environmental Science and Pollution Research* 27 (2020): 24284–24298.

28. C. Galletti, M. Dosa, N. Russo, and D. Fino, "Zn^{2+} and Cd^{2+} Removal from Wastewater Using Clinoptilolite as Adsorbent," *Environmental Science and Pollution Research* 28 (2021): 24355–24361.

29. L. Habte, N. Shiferaw, M. D. Khan, T. Thriveni, and J. W. Ahn, "Sorption of Cd^{2+} and Pb^{2+} on Aragonite Synthesized from Eggshell," *Sustainability* 12 (2020): 1174.

30. V. Uwamariya, B. Petrusevski, P. Lens, and G. L. Amy, "Effect of pH and Calcium on the Adsorptive Removal of Cadmium and Copper by Iron Oxide–Coated Sand and Granular Ferric Hydroxide," *Journal of Environmental Engineering* 142 (2016): C4015015.

31. A. Dişbudak, S. Bektaş, S. Patır, Ö. Genç, and A. Denizli, "Cysteine-Metal Affinity Chromatography: Determination of Heavy Metal Adsorption Properties," *Separation and Purification Technology* 26 (2002): 273–281.

32. S. Moulay and N. Bensacia, "Removal of Heavy Metals by Homolytically Functionalized Poly(acrylic acid) with Hydroquinone," *International Journal of Industrial Chemistry* 7 (2016): 369–389.

33. N. Candan, N. Tüzmen, M. Andac, C. A. Andac, R. Say, and A. Denizli, "Cadmium Removal out of Human Plasma Using Ion-Imprinted Beads in a Magnetic Column," *Materials Science and Engineering: C* 29 (2009): 144–152.

34. M. Karbarz, A. M. Khalil, K. Wolowicz, K. Kaniewska, J. Romanski, and Z. Stojek, "Efficient Removal of Cadmium and Lead Ions From Water by Hydrogels Modified with Cystine," *Journal of Environmental Chemical Engineering* 6 (2018): 3962–3970.

35. B. Pan, H. Qiu, B. Pan, et al., "Highly Efficient Removal of Heavy Metals by Polymer-Supported Nanosized Hydrated Fe(III) Oxides: Behavior and XPS Study," *Water Research* 44 (2010): 815–824.

36. F. Ge, M.-M. Li, H. Ye, and B.-X. Zhao, "Effective Removal of Heavy Metal Ions Cd^{2+}, Zn^{2+}, Pb^{2+}, Cu^{2+} from Aqueous Solution by Polymer-Modified Magnetic Nanoparticles," *Journal of Hazardous Materials* 211 (2012): 366–372.

37. A. Shahbazi, H. Younesi, and A. Badiei, "Functionalized SBA-15 Mesoporous Silica by Melamine-Based Dendrimer Amines for Adsorptive Characteristics of Pb(II), Cu(II) and Cd(II) Heavy Metal Ions in Batch and Fixed Bed Column," *Chemical Engineering Journal* 168 (2011): 505–518.

38. M. Mansour, M. Ossman, and H. Farag, "Removal of Cd (II) ion from Waste Water by Adsorption onto Polyaniline Coated on Sawdust," *Desalination* 272 (2011): 301–305.

39. Y. Liu, L. Hu, B. Tan, et al., "Adsorption Behavior of Heavy Metal Ions from Aqueous Solution onto Composite Dextran-Chitosan Macromolecule Resin Adsorbent," *International Journal of Biological Macromolecules* 141 (2019): 738–746.

40. E. Abdel-Halim and S. S. Al-Deyab, "Preparation of Poly(acrylic acid)/Starch Hydrogel and Its Application for Cadmium Ion Removal from Aqueous Solutions," *Reactive and Functional Polymers* 75 (2014): 1–8.

41. W.-B. Wang, D.-J. Huang, Y.-R. Kang, and A.-Q. Wang, "One-Step *in situ* Fabrication of a Granular Semi-IPN Hydrogel Based on Chitosan and Gelatin for Fast and Efficient Adsorption of Cu^{2+} Ion," *Colloids and Surfaces B, Biointerfaces* 106 (2013): 51–59.

42. L. R. Rad, A. Momeni, B. F. Ghazani, M. Irani, M. Mahmoudi, and B. Noghreh, "Removal of Ni^{2+} and Cd^{2+} Ions from Aqueous Solutions Using Electrospun PVA/Zeolite Nanofibrous Adsorbent," *Chemical Engineering Journal* 256 (2014): 119–127.

43. N. A. Qasem, R. H. Mohammed, and D. U. Lawal, "Removal of Heavy Metal Ions from Wastewater: A Comprehensive and Critical Review," *npj Clean Water* 4 (2021): 36.

44. M. Nakahata, A. Sumiya, Y. Ikemoto, et al., "Hyperconfined Bio-Inspired Polymers in Integrative Flow-Through Systems for Highly Selective Removal of Heavy Metal Ions," *Nature Communications* 15 (2024): 5824.

45. S. Y. Park, J. H. Yoon, C. S. Hong, et al., "A Pyrenyl-Appended Triazole-Based Calix[4]arene as a Fluorescent Sensor for Cd^{2+} and Zn^{2+}," *Journal of Organic Chemistry* 73 (2008): 8212–8218.

46. A. Manceau, P. Bustamante, A. Haouz, et al., "Mercury(II) Binding to Metallothionein in Mytilus Edulisrevealed by High Energy-Resolution XANES Spectroscopy," *Chemistry—A European Journal* 25 (2019): 997–1009.

47. E. Chekmeneva, R. Prohens, J. M. Díaz-Cruz, C. Ariño, and M. Esteban, "Thermodynamics of Cd^{2+} and Zn^{2+} Binding by the Phytochelatin $(\gamma\text{-Glu-Cys})_4$-Gly and Its Precursor Glutathione," *Analytical Biochemistry* 375 (2008): 82–89.

48. Y. Cheng, Y.-B. Yan, and J. Liu, "Spectroscopic Characterization of Metal Bound Phytochelatin Analogue $(Glu–Cys)_4$–Gly," *Journal of Inorganic Biochemistry* 99 (2005): 1952–1962.

49. K. Viswanathan, M. H. Schofield, I. Teraoka, and R. A. Gross, "Surprising Metal Binding Properties of Phytochelatin-Like Peptides Prepared by Protease-Catalysis," *Green Chemistry* 14 (2012): 1020–1029.

Supporting Information

Additional supporting information can be found online in the Supporting Information section.